

SANDIA REPORT

SAND2006-0995
Unlimited Release
Printed March 2006

Ion-Induced Gammas for Photofission Interrogation of HEU

Arlyn Antolak, Barney Doyle, Daniel Morse, Paula Provencio

Prepared by
Sandia National Laboratories
Albuquerque, New Mexico 87185 and Livermore, California 94550

Sandia is a multiprogram laboratory operated by Sandia Corporation,
a Lockheed Martin Company, for the United States Department of Energy's
National Nuclear Security Administration under Contract DE-AC04-94AL85000.

Approved for public release; further dissemination unlimited.



Sandia National Laboratories

Issued by Sandia National Laboratories, operated for the United States Department of Energy by Sandia Corporation.

NOTICE: This report was prepared as an account of work sponsored by an agency of the United States Government. Neither the United States Government, nor any agency thereof, nor any of their employees, nor any of their contractors, subcontractors, or their employees, make any warranty, express or implied, or assume any legal liability or responsibility for the accuracy, completeness, or usefulness of any information, apparatus, product, or process disclosed, or represent that its use would not infringe privately owned rights. Reference herein to any specific commercial product, process, or service by trade name, trademark, manufacturer, or otherwise, does not necessarily constitute or imply its endorsement, recommendation, or favoring by the United States Government, any agency thereof, or any of their contractors or subcontractors. The views and opinions expressed herein do not necessarily state or reflect those of the United States Government, any agency thereof, or any of their contractors.

Printed in the United States of America. This report has been reproduced directly from the best available copy.

Available to DOE and DOE contractors from
U.S. Department of Energy
Office of Scientific and Technical Information
P.O. Box 62
Oak Ridge, TN 37831

Telephone: (865)576-8401
Facsimile: (865)576-5728
E-Mail: reports@adonis.osti.gov
Online ordering: <http://www.osti.gov/bridge>

Available to the public from
U.S. Department of Commerce
National Technical Information Service
5285 Port Royal Rd
Springfield, VA 22161

Telephone: (800)553-6847
Facsimile: (703)605-6900
E-Mail: orders@ntis.fedworld.gov
Online order: <http://www.ntis.gov/help/ordermethods.asp?loc=7-4-0#online>



Ion-Induced Gammas for Photofission Interrogation of HEU

Arlyn Antolak, Daniel Morse
Engineered Materials Department
Sandia National Laboratories
P.O. Box 969
Livermore, CA 94551

Barney Doyle, Paula Provencio
Radiation-Solids Interactions Department
Sandia National Laboratories
P.O. Box 5800
Albuquerque, New Mexico 87185

Abstract

High-energy photons and neutrons can be used to actively interrogate for heavily shielded special nuclear material (SNM), such as HEU (highly enriched uranium), by detecting prompt and/or delayed induced fission signatures. In this work, we explore the underlying physics for a new type of photon source that generates high fluxes of mono-energetic gamma-rays from low-energy (<500 keV) proton-induced nuclear reactions. The characteristic energies (4- to 18-MeV) of the gamma-rays coincide with the peak of the photonuclear cross section. The source could be designed to produce gamma-rays of certain selected energies, thereby improving the probability of detecting shielded HEU or providing a capability to determine enrichment inside sealed containers. The fundamental physics of such an interrogation source were studied in this LDRD through scaled ion accelerator experiments and radiation transport modeling. The data were used to assess gamma and neutron yields, background, and photofission-induced signal levels from several (p,γ) target materials under consideration.

Contents

1. INTRODUCTION	5
2. SYSTEM DEVELOPMENT	6
2.1 Neutron Tube Source	6
2.2 Gamma Tube Concept	7
2.2.1 Coaxial Gamma Source	8
2.2.2 Axial Gamma Source	9
2.2.3 Scalable Linear Source	10
3. ACCELERATOR EXPERIMENTS	12
3.1 Gamma Yields	13
3.2 Photofission Signatures	14
4. MODELING	17
5. SUMMARY	18
6. REFERENCES	19

Figures

Figure 1. Coaxial neutron generator producing 10^{11} neutrons/s.	7
Figure 2. Schematic of the gamma tube using the $^{11}\text{B}(\text{p},\gamma)^{12}\text{C}$ reaction resonance at 163-keV proton energy.....	8
Figure 3. Schematic showing a conceptual axial acceleration gamma tube	9
Figure 4. Two generator units connected together with both units sharing the RF-amplifier and the matching circuit, vacuum pump, and the high voltage supply	10
Figure 5. Photo on left shows the Radiation Cell Facility with remotely operated ion accelerators. Schematic on right shows experimental setup for measuring gamma yields, background levels, and photofission signals	12
Figure 6. Spectra from candidate gamma tube target materials collected with a 5 inch x 5 inch NaI detector at different incident proton energies	13
Figure 7. Measured total gamma-ray yields from LiF and B ₄ C as a function of incident proton energy.	14
Figure 8. Delayed gamma-ray spectra from pulsed photofission experiments of ^{238}U	15

Tables

Table 1. Candidate gamma tube low-energy (p,γ) target isotopes	9
--	---

1. INTRODUCTION

Every year approximately 6 million maritime cargo containers are delivered to U.S. ports. Due to the size and complexity of their cargo, these containers offer a variety of opportunities for smuggling different kinds of contraband, including the possibility of a nuclear weapon or the components to assemble one. Failure to detect a concealed nuclear weapon or improvised nuclear device would lead to major physical damage and loss of life in a U.S. urban center and major economic and psychological damage throughout the entire U.S. At present, only a small fraction of containers are inspected beyond a routine document screening, although passive detection and radiographic imaging systems are becoming more commonplace at the nation's largest ports. The drawback to passive inspection is that the natural radioactive emissions from even large amounts of fissile materials can either be easily shielded (by the surrounding cargo or intentionally emplaced shielding) or are difficult to detect (due to background, short collection times, and poor statistics). A more reliable approach is to actively interrogate for the nuclear material with high-energy neutrons and/or photons to induce fission signals (neutrons and gamma-rays) that are detectable through cargo or other shielding materials. Thus, an interrogation source capable of producing *both* neutrons and photons is optimal because neutrons readily penetrate intermediate and high atomic number materials, while photons are useful when the intervening materials are hydrogenous or contain neutron absorbers. Ideally, an interrogation system can perform with high detection probability, low false alarm rates, and without impeding container traffic. To satisfy these requirements, the interrogation system must incorporate a very intense source (producing $>10^{10}$ particles/s) so that reliable screenings can be completed within minutes or less.

In this LDRD project, we explored the underlying physics of a conceptual Gamma Tube source. Unlike conventional particle accelerator technology, this source uses the lowest-energy proton-induced nuclear reactions to make high-energy gamma-rays, either in pulsed or DC mode. As a result, the source would be simpler, more cost effective, more efficient, and easier to scale than comparable high-energy particle accelerator alternatives. Additionally, since high-energy monochromatic gamma-rays result in lower personnel radiation doses, the proposed system will satisfy existing federal regulations that limit other active interrogation approaches. We assessed the viability of this source through a program of experiments and simulations that determined the performance limits of a field-deployable interrogation system which we call FIND for "Fissmat Inspection for Nuclear Detection". Our research approach involves 1) establishing the scientific basis and underlying materials science required in the design of the source and associated (p,γ) reaction targets, 2) performing analyses to evaluate configurations and operational parameters for the FIND system, and 3) validating the simulation models from scaled-down accelerator experiments conducted in the Sandia High Radiation Laboratory. The results of these experiments and simulations will define the parameter space over which this cargo container inspection technology is practical.

2. SYSTEM DEVELOPMENT

The FIND system requires high fluences of high-energy gamma-rays for active interrogation of shielded fissile materials. Our approach is to develop a source that uses nuclear reactions of such a low energy (<500 keV) that they can be reached by a simple Gamma Tube, thus eliminating the need for a more costly and complex ion accelerator. We call this use of low-energy nuclear reactions to produce high energy radiation nature's (nuclear) amplifier. The operational basis for the system is drawn from the rf-plasma neutron generators recently developed at Lawrence Berkeley National Laboratory (LBNL) and described below [1].

2.1 Neutron Tube Source

Although isotopic sources release neutrons by radioactive decay, their intensities are generally too low to be suitable for a cargo container active interrogation system. At the other extreme, the most intense sources of neutrons are from nuclear fission reactors or high-energy particle accelerators (the latter "spallation sources" use proton beams to break up heavy nuclei in a target). These large, complex, and costly installations yield copious amounts of neutrons at energies up to hundreds of millions of electron volts, but would be impractical to operate and maintain as part of an active interrogation system at a seaport facility. High intensities of neutrons can also be produced by a neutron tube (generator) which essentially is a miniature, low-energy accelerator that produces neutrons by hitting a metal target with deuterium or tritium ions. A fusion reaction occurs between the deuterium in the beam and deuterium or tritium in the target (D-D or D-T reactions) resulting in a high flux of energetic neutrons. One of the drawbacks in typical commercial units is the short operational lifetime due to the target becoming depleted of the hydrogen isotopes.

Many of the limitations in conventional neutron tube sources have been recently overcome in a new generator design developed at LBNL. This system uses a miniature-ized plasma ion source, driven by a radio-frequency antenna, to efficiently produce a high current of deuterium ions (see Figure 1). More than 90 percent of the deuterium ions in the plasma are monoatomic with energies at the peak of the reaction cross section compared to other tubes which typically only have about 20 percent mono-atomic ions. The neutron output is further enhanced as a result of the system's coaxial cylindrical tube design in which the cylinder-shaped ion source emits beams radially along its length, striking a large area target wrapped around it. The target in the LBNL neutron tube consists of a thin sheet of titanium bonded to a copper substrate with water-cooling channels. As the beam hits the target, new deuterium ions are being continually added, so the target does not become depleted. Further, neutron production can be increased simply by extending the length of the cylinder (tube). The highest yield system has achieved intensities of 10^{11} n/s.

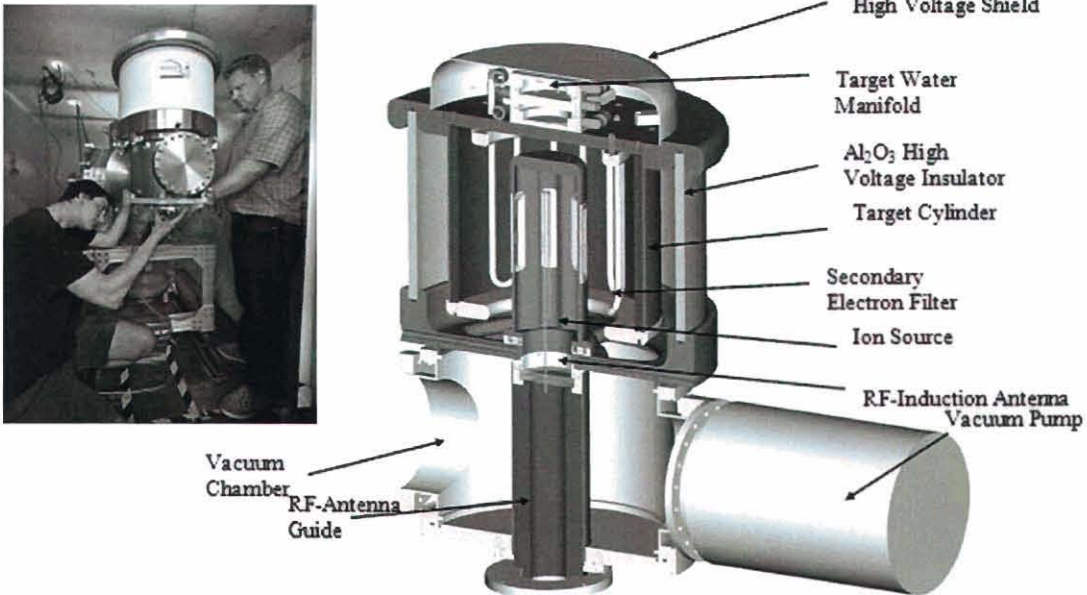


Figure 1. Coaxial neutron generator producing 10^{11} neutrons/s. The generator operates at 120 kV and 350 mA with 40 kW of beam power at the target. The generator is about 40 cm in diameter and 80 cm tall excluding power supplies and vacuum pumps.

2.2 Gamma Tube Concept

An analogue Gamma Tube has been conceptualized that is capable of generating an ampere or more current of a few hundred keV-energy protons which bombard a cylindrical extraction electrode target rich in the isotope that produces the (p, γ) nuclear reaction. There are some features in the existing LBNL neutron generator design that would remain the same for the gamma source. For example, rf-induction is a powerful way of generating high current (> 1 Ampere) proton beams having a high fraction of protons (easily more than 90% of the total hydrogen beam including the other two species, H_2^+ and H_3^+). To ensure reliable high voltage operation the gamma-ray tube would also be vacuum pumped. With reasonable pumping, the pressure would drop to the 10^{-4} Torr range, which allows trouble free high voltage operation. The ion source is protected from the secondary electrons with a filter rod structure; this prevents high-energy electrons from accelerating back to the source and potentially over-heating it. The protection from the secondary electrons is especially important in the case of the gamma source. Due to the fairly small cross-section of some of the nuclear reactions at these proton energies, the generator has to run at fairly high current which means the ion beam power at the target can be of the order of 200 kW. Although the large surface area of the target helps to dissipate the thermal load, higher power operation of the gamma source will also require new designs for the ion source and the cooling system used for the neutron tube.

2.2.1 Coaxial Gamma Source

A co-axial gamma-tube design has several advantages that would carry over from the neutron tube system. The advantages include (i) the capability to produce high beam current, (ii) better cooling, (iii) simpler design, (iv) compact design, and (v) more spatially uniform photon flux. Figure 2 shows a schematic of a conceptual coaxial type gamma source that is very similar to the neutron tube described above. The ion source, located at the center of the gamma generator, is hydrogen plasma formed by rf-induction discharge. The antenna is water-cooled copper tubing enclosed inside a quartz tube.

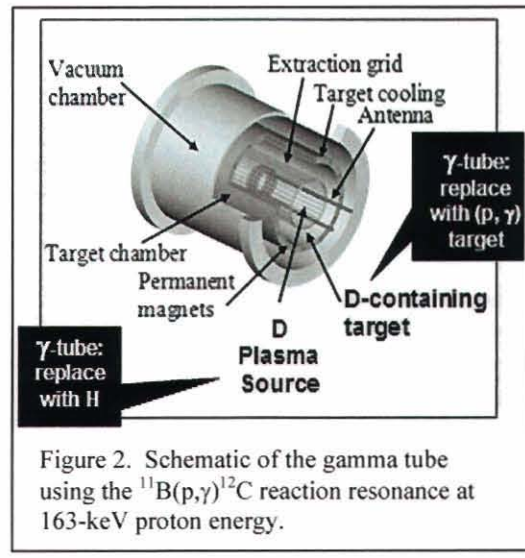


Figure 2. Schematic of the gamma tube using the $^{11}\text{B}(\text{p},\gamma)^{12}\text{C}$ reaction resonance at 163-keV proton energy.

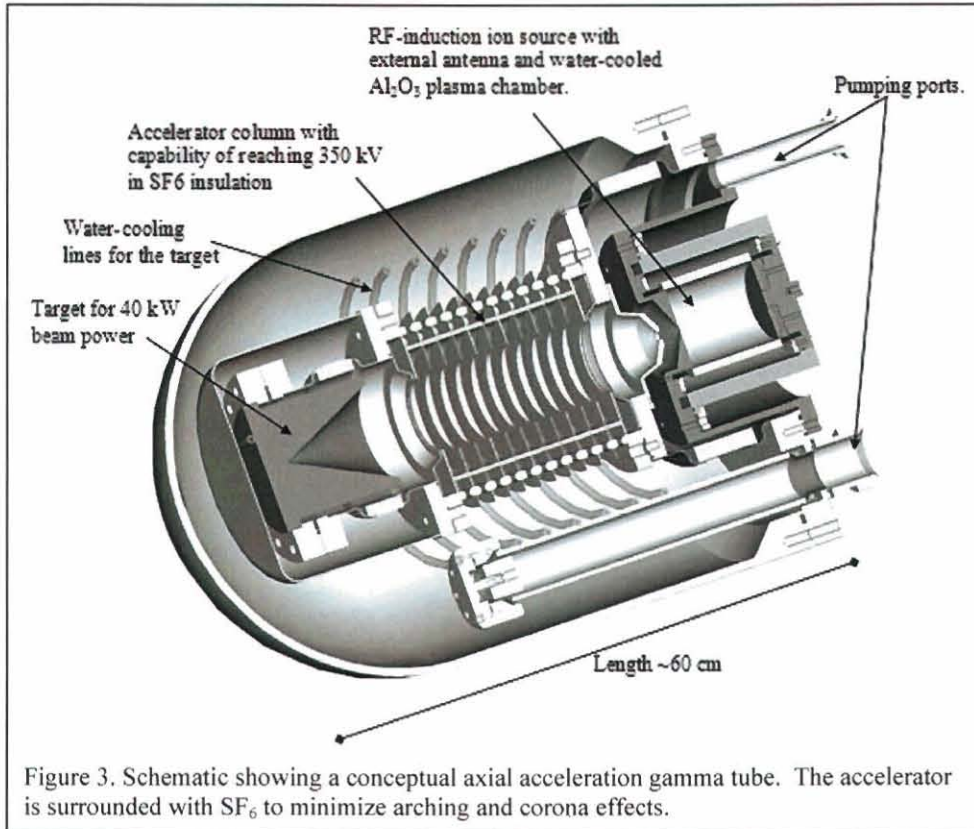
For the (p,γ) target material, Table 1 lists four promising low-energy nuclear reactions that produce gamma-rays with energies greater than 6-MeV (the photofission threshold energy is approximately 5.5-MeV) [2-8]. Of these, the 163-keV ^{11}B and 203-keV ^{27}Al reactions offer the most direct path to a gamma tube system based on the existing co-axial neutron generator technology. Suitable target materials for these reactions include LaB_6 or B_4C (for p-B) and Al (for p-Al) which are easy to fabricate and also have good thermal, electrical, and mechanical properties [9]. For example, lanthanum hexaboride (LaB_6) is a rigid ceramic with good thermal shock resistance and good chemical and oxidation resistance. It also has high electron emissivity and good electrical conductivity. As a result, it is commonly used as a cathode material in electron microscopes. Similarly, boron carbide (B_4C) is one of the hardest materials known, ranking third behind diamond and cubic boron nitride. It has very good chemical resistance, good nuclear properties (commonly used as a neutron absorber in reactors), and has low density (2.52 g/cm³). B_4C can be formed as a coating on a suitable substrate by vapor phase reaction techniques, e.g., using boron halides or di-borane with methane or another chemical carbon source. The main drawback with both the ^{11}B and ^{27}Al is their low (p,γ) reaction cross sections, necessitating the need to operate the gamma tube at high current to increase the source output. For example, in a boron-based interrogation system, a coaxial source producing an ampere of proton current at the 163-keV reaction resonance (0.157 mb) will only generate a fluence of about 6×10^8 γ/s. The next boron resonance occurs at higher proton energy (675-keV), but its cross section is smaller (0.05 mb) and much wider (322 keV). Similarly, the reaction for aluminum at a proton energy of 203-keV has a cross section of less than 0.03 mb.

Table 1. Candidate gamma tube low-energy (p,γ) target isotopes.

Reaction	Gamma-Ray Energy (MeV)	Cross Section (mb)	Proton Energy (keV)	Width (keV)	Target Fabrication
$^{11}\text{B}(p,\gamma)^{12}\text{C}$	11.7	0.157	163	7	Easy
$^{19}\text{F}(p,\alpha\gamma)^{16}\text{O}$	6.13	160	340	3	Difficult
$^7\text{Li}(p,\gamma)^8\text{Be}$	14.8, 17.7	6	441	12	Moderate
$^{27}\text{Al}(p,\gamma)^{28}\text{Si}$	9.8, 11.5	<0.03 150	203 632	>0.005 0.007	Easy

2.2.2 Axial Gamma Source

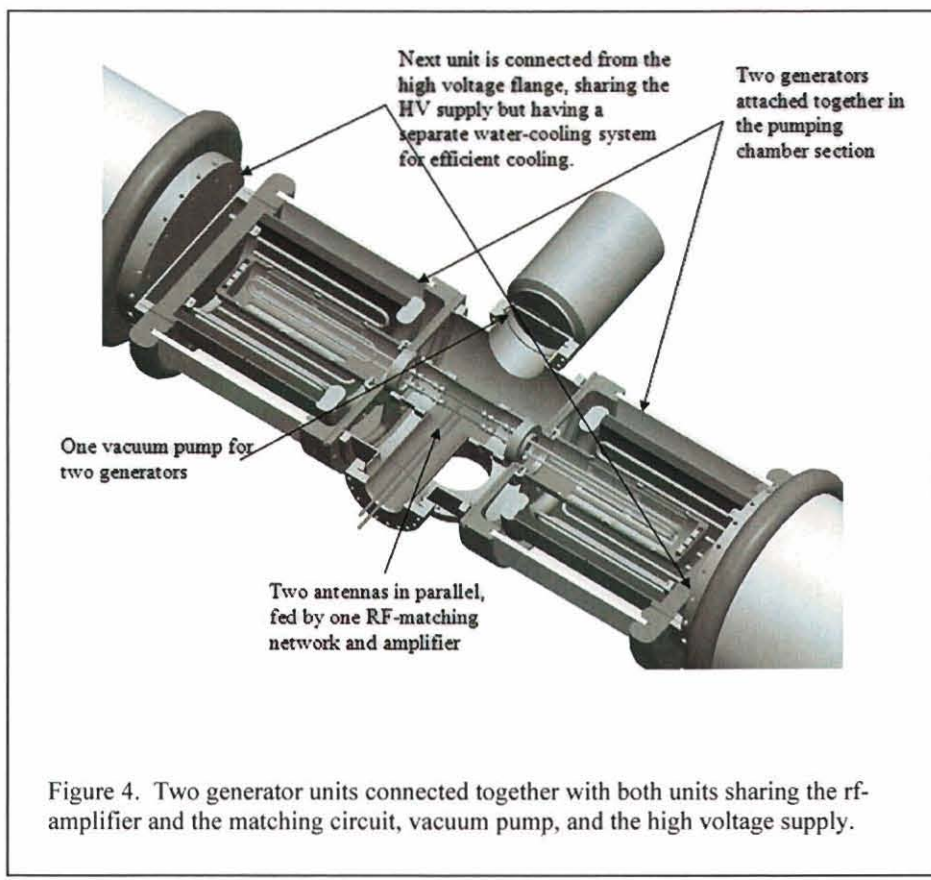
The other (p,γ) reactions in Table 1 have larger reaction cross sections, but also require scaling the gamma tube source voltage to higher proton energies. On the other hand, it may not be possible to readily scale the above coaxial tube design to higher proton voltages (without going to much larger tube diameters). To achieve higher energies, we are considering an analogous design based on a simple axial accelerator column concept. In this system, the protons are first produced in an rf-driven plasma source and then extracted and accelerated to their full energy using a simple electrostatic accelerator column (see Figure 3). The accelerated protons then impinge on a water-cooled, V-shaped target (rather than a cylindrical tube target as in the coaxial design).



The axial gamma tube is vacuum pumped to minimize the electrons produced by ionizing the gas in the beam path. Sulfur hexafluoride gas is also used to minimize corona and arcing in the column when operating at these high voltages. Another factor in the development of this type of gamma tube source is that fewer target materials are available that are both high in abundance of fluorine or lithium isotopes and also have suitable electrical, thermal, and fabrication properties.

2.2.3 Scalable Linear Source

A significant advantage of the source design is its potential to scale to almost any length by stacking together individual base units. For example, the coaxial gamma tube can be taken to an order of magnitude higher power level by stacking ten of the 1-Ampere systems together. In the base units, the lower vacuum plate is in ground potential and the upper one is at the target potential (e.g., ~165-kV for the p-B reaction). These sources can be stacked on top of each other in a sequence, where two high voltage flanges are shared in one end of the two generators and, on the other end, the pumping chamber is shared with another generator. In this way, only five high voltage feeds, five vacuum pumps and five rf-systems are needed to operate the stack of ten generators. This concept is depicted in Figure 4 where the two coaxial sources are attached by a single pumping chamber and high voltage flange.



The final source system integrates these gamma-ray tubes to produce a new active interrogation source. Owing to its linear scalability, the photon source will be well-suited for many diverse applications ranging from very large fixed site interrogation systems to intermediate-size mobile or remote inspection systems to compact systems for assaying the internal contents of hazardous waste drum containers.

3. ACCELERATOR EXPERIMENTS

In this section, we focus on experiments related to gamma-ray production and photofission for the gamma tube source since the issues for developing and implementing the neutron tube part have previously been described [1]. The photofission cross section for most nuclear materials has a peak that extends from approximately 5-MeV to 20-MeV. In particular, the peak for ^{235}U is at 13.8-MeV with a full-width-at-half-maximum of 5-MeV and a threshold of 5.8-MeV. Ideally, we would like to select nuclear reactions that produce gamma-rays having their energy near the peak of the cross section. However, as the gamma-ray energy is increased above 7.5-MeV (the average nuclear binding energy), there can be also be an associated increase in the background signal due to the production of photoneutrons from surrounding materials or from Compton scattered source photons. Experiments are being performed on a remotely operated 700-keV Van de Graaff ion accelerator system in the Sandia High radiation Lab to assess the above issues and to evaluate the operational performance of the Gamma Tube. Figure 5 shows a photograph of the accelerator which is physically located inside a high radiation cell having 1-2 foot thick concrete walls and ceiling for shielding. The low-energy accelerator in the front of the photograph is also part of the ion beam system, but is not used in the present experiments. In addition to protons, other ions such as deuterium, ^3He , and ^4He are also routinely accelerated in this facility. For the present experiments, a 1-10 micro-Ampere beam of up to 700-keV protons bombards a target attached to a water-cooled stage producing mono-energetic gamma-rays from low-energy nuclear reactions (see schematic in Figure 5 for experimental arrangement). Two NaI detectors are used both to monitor the intensity of gamma-rays produced by the target and to detect the prompt or delayed gammas induced by photofission; a ^3He detector array is used to count prompt or delayed neutron signals produced by photofission events. Other materials can be placed between the gamma source and nuclear material to simulate intervening cargo or various types of shielding, as well as to measure the background caused by photoneutrons or scattered gamma-rays.

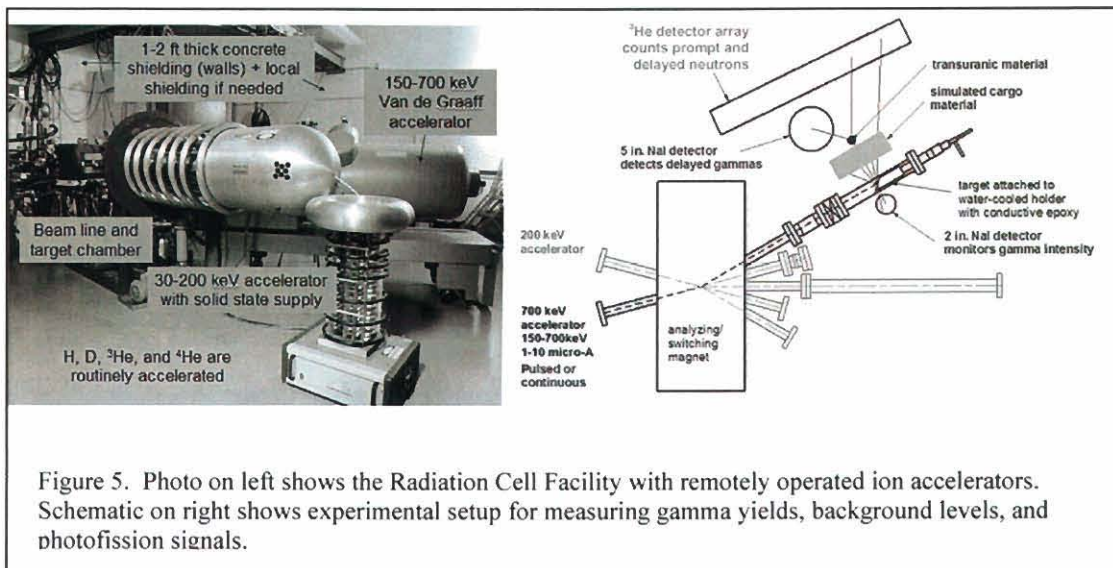


Figure 5. Photo on left shows the Radiation Cell Facility with remotely operated ion accelerators. Schematic on right shows experimental setup for measuring gamma yields, background levels, and photofission signals.

3.1 Gamma Yields

Various target materials were tested to determine the corresponding gamma yields and energy spectra over a range of proton energies. Figure 6 shows gamma spectra collected from LiF, Teflon, B₄C, and Mg bombarded with a continuous beam of protons. Each spectrum was collected with a 5-inch NaI detector and normalized to 1- μ C of charge. The (p, γ) target to detector distance was set at 7 cm. Both boron carbide and magnesium have rather low gamma-ray yield which is consistent with the reported ¹¹B cross section value given in Table 1. Magnesium was tested because we could not find a value for its cross section in the literature, but it was reported that a 6.19-MeV gamma-ray (in addition to 4.86-MeV and 0.82-MeV gammas) is produced corresponding to the 317-keV resonance of the ²⁵Mg(p, γ)²⁶Al reaction [2]. While our spectra clearly show the 6.19-MeV gamma-ray, we also see gammas that arise from the higher energy (~8-MeV) branching channels that can occur for the ²⁶Mg(p, γ)²⁷Al reaction. The LiF and Teflon spectra are dominated by the characteristic 6.13-MeV fluorine gamma-ray which was even observed for 250-keV protons from the accelerator (fluorine has a small resonant cross section of ~0.2 mb at 224-keV proton energy). As indicated in Table 1, the resonant reaction for lithium occurs at 441-keV which accounts for the significant jump in the measured yield between the 350-keV and 450-keV spectra. The ⁷Li reaction is of interest because it produces 17.64-MeV (63% emission/reaction) and 14.74-MeV (37% emission/reaction) gamma-rays which also coincide well with the peak of the photofission cross section. There also appears to be an unidentified, weak low-energy nuclear reaction in Teflon that produces ~12-MeV gammas and may be due to a trace impurity in the material.

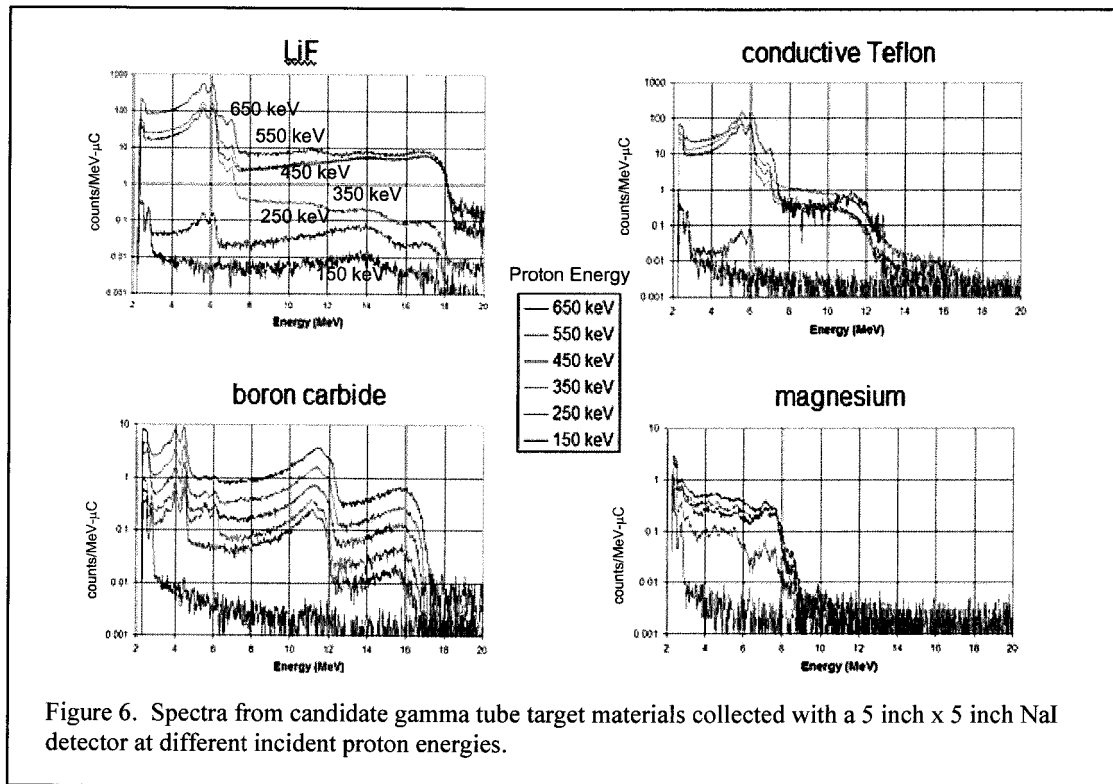


Figure 6. Spectra from candidate gamma tube target materials collected with a 5 inch x 5 inch NaI detector at different incident proton energies.

The spectra from the LiF and B₄C target samples were further analyzed to quantify the total gamma-ray yield as a function of incident proton energy corresponding to each (p,γ) isotope, i.e., ⁷Li, ¹⁹F, and ¹¹B. The results are plotted in Figure 7 with the assumption that the NaI gamma detector had an absolute efficiency of 15% at all energies. These data indicate that the recommended 10¹⁰ particles/s intensity threshold cannot be achieved with ¹¹B even when the source is operating at 1-Ampere proton current. On the other hand, this intensity can be achieved (shaded region of the plot) for both F and Li (marginally) reactions, but operation at higher proton energies and currents is required.

3.2 Photofission Signatures

Active interrogation relies on stimulating nuclear material to produce radiation signals that can then be detected through intervening shielding material. In gamma-based systems, some fraction of the mono-energetic source gammas will be shifted to lower energies by Compton-scattering and pair production as they pass through intervening material. This has the effect of reducing the total fluence of “photofission-worthy” gammas at the nuclear material being interrogated, resulting in a lower detectable signal. The reduced signal can be partially ameliorated by 1) using nuclear reactions that produce gammas with energies >10-MeV so that some of the scattered photons will have sufficiently high energies to still induce photofission and 2) any photonuclear events that occur with

surrounding materials produce energetic neutrons that can also induce fission. An effective active interrogation system must be able to maximize and distinguish the prompt and/or delayed fission signals from the neutron and gamma background that arises from other surrounding materials. For example, the prompt neutron signal can be affected by the photoneutron background caused when the source gammas interact with materials near the object being interrogated. Fortunately, the neutron production cross sections of most nuclear materials are much higher than that of common materials so the neutron background in gamma-based interrogation techniques is fairly low.

We have performed preliminary (p, γ) accelerator experiments to detect prompt neutrons and delayed gammas from photo-fission. Figure 8 shows a plot of the data from one of the experiments that measured the delayed gamma spectra from a pulsed gamma source. The proton beam from the accelerator was pulsed electrostatically at 5 kHz with a 50%

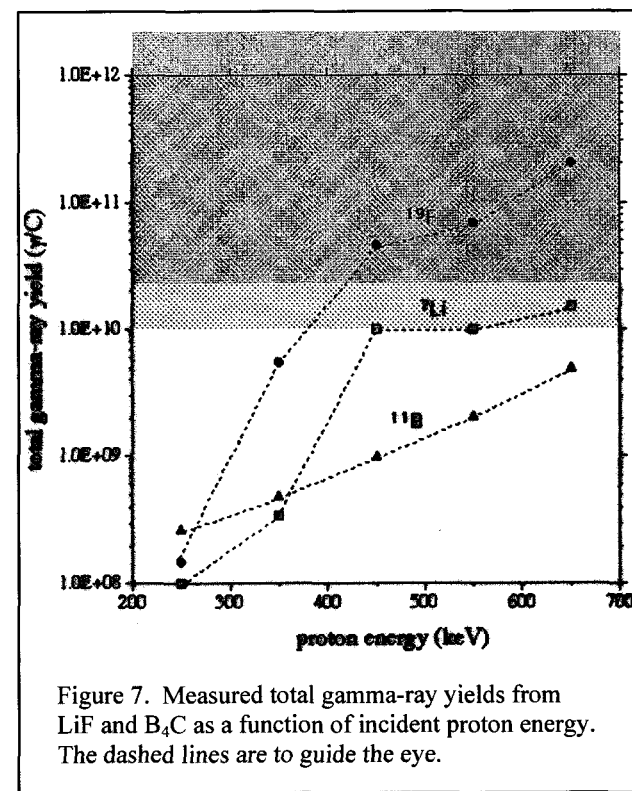


Figure 7. Measured total gamma-ray yields from LiF and B₄C as a function of incident proton energy. The dashed lines are to guide the eye.

duty cycle (on 100 μ s and off 100 μ s) by applying a 500 volt square wave to 75-cm long deflection plates spaced 2.5-cm apart. The 450-keV protons bombarded a LiF target located inside a 1.5-inch diameter beamline tube, thereby producing 6 (F), 15 (Li), and 18 (Li) MeV gamma-rays. A large fraction of these gammas struck the depleted uranium sample which consisted of seven 50 mm diameter x 3 mm thick discs (780 g ^{238}U) that were stacked outside of the beamline tube 2-cm from the LiF target. A 5" x 5" NaI gamma detector was positioned 13-cm from the LiF target on the opposite side of the ^{238}U . The detector was electronically gated with a 35% duty cycle (on 20 μ s after proton beam off and off 10 μ s before proton beam on) to capture the short-lived delayed gammas and to avoid any interferences from the source gamma-rays. Beneath the gamma source-uranium disc experimental arrangement was a plastic-moderated ^3He neutron detector array to record the prompt neutron signal. Each photofission-induced gamma-ray spectrum was collected for 100 seconds with 6- μA peak (3- μA average) proton current.

Figure 8a shows the photofission spectra collected at three proton beam energies (300, 400, and 500 keV) with and without ^{238}U present. Figure 8b shows the results obtained when each spectrum without ^{238}U was subtracted from the corresponding spectrum with ^{238}U present. Performing this subtraction automatically removes background contributions such as due to Bremsstrahlung or detector effects. The integrated net signal between 300-keV and 400-keV is computed to be 160 counts/sec and corresponds to the count rate due primarily to the fluorine reaction at the 340-keV cross section resonance. Likewise, the increase in net signal between 400-keV and 500-keV spectra (98 counts/sec) results mainly from the Li reaction at the 441-keV resonance. Additional experiments are underway to measure the delayed gamma-ray spectra in the 2- to 6-MeV range.

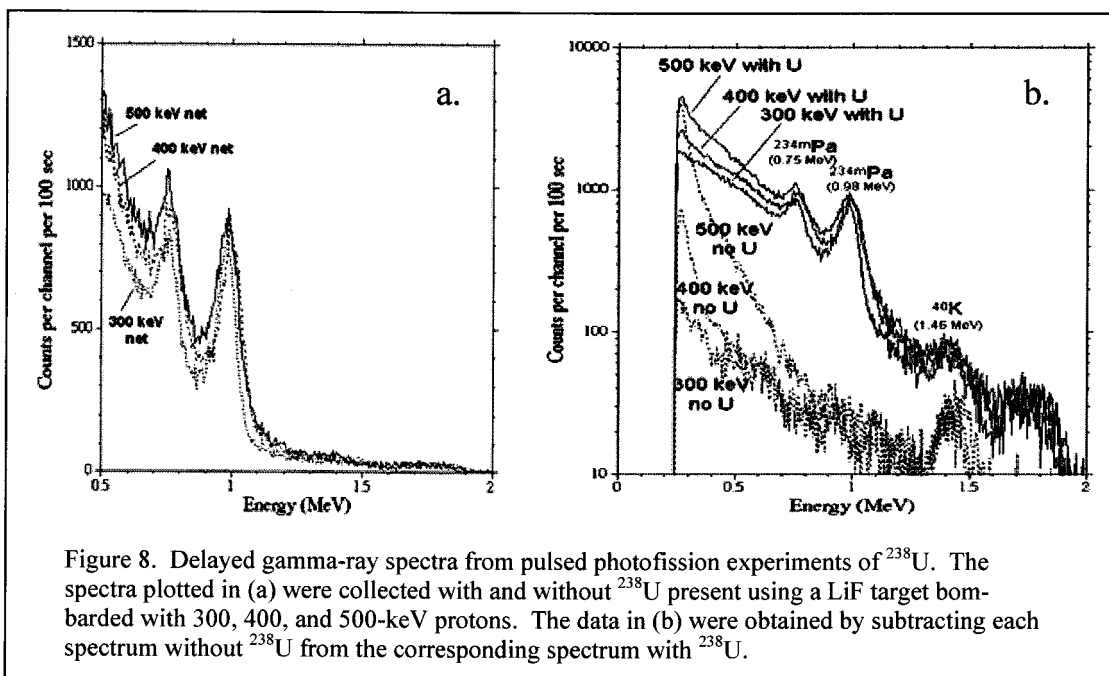


Figure 8. Delayed gamma-ray spectra from pulsed photofission experiments of ^{238}U . The spectra plotted in (a) were collected with and without ^{238}U present using a LiF target bombarded with 300, 400, and 500-keV protons. The data in (b) were obtained by subtracting each spectrum without ^{238}U from the corresponding spectrum with ^{238}U .

For active interrogation, utilizing delayed gamma-rays in this latter energy range has the additional benefit that normal radioactive background almost never produces gamma-rays above 3-MeV and, thus, does not interfere with this signature [10]. Cumulative neutron and gamma count rate results are given in Table 2 along with the net photofission signal in each case. While the signal-to-background ratios are rather low, the results are nevertheless quite encouraging. For instance, the photonuclear cross sections for both depleted and highly enriched uranium (^{235}U) are approximately the same at 6-MeV (p-F reaction), but the ^{235}U cross section is approximately 2.5 times greater than ^{238}U at 15-MeV (p-Li reaction) [11]. Further, ^{238}U has a significant gamma-ray decay background which is almost non-existent for ^{235}U . Both these effects will improve the signal-to-background ratio for detecting ^{235}U signatures. Additional experiments could be performed to optimize the data collection process (pulse rates), signal detection, and, as stated earlier, assess the background levels by also inserting different materials between the gamma source and radiation detectors.

4. MODELING

A simple, compact, and low-cost source design is important for the wide deployment of FIND interrogation systems at seaports or border crossing inspection stations. In one suggested inspection system concept-of-operation, the source is located in underground to shield the excess radiation to inspection workers. A cargo container is towed (transported) over the collimated fan beam of source neutrons and/or gamma-rays which cause fission in any nuclear material that may be present. Large arrays of neutron and gamma detectors are positioned around the cargo container to detect the fission emission signatures. An optional low exposure radiographic screening of the container's contents could also be performed using the Gamma Tube source and an array of gamma detectors to record the transmission image. Because of its scalability, it would also be possible to replace the fan beam "point" source with a "line" source that extends over the entire (20 foot) length of the container. In this latter case, the cylindrical wedge-shaped beam from the line source illuminates the entire container at one time, as compared to the fan beam configuration where only a thin slice of cargo is illuminated as a container moves rapidly past it.

An optimal design for a field deployable FIND system requires an assessment of the most useful radiation signatures, the best detectors and data collection methods, and the most advanced signal processing. In parallel with the above accelerator experiments, we are evaluating the FIND system in terms of its "detectability" performance using a "zeroth-order" analytical model that captures the essential nuclear and transport effects, but does not include the detailed, and more computationally intensive, models found in advanced radiation transport codes. Since other studies have examined the performance of neutron- and bremsstrahlung-based sources for active interrogation of lightly or unshielded nuclear material [12-16], our focus has been on determining the detectability of fission signatures in different shielding scenarios using the mono-energetic gamma-rays from our tube source. We are using the above experimental results to validate the model predictions and then plan to extend the calculations to model the performance of a full-scale FIND system. Preliminary simulation results suggest that 0-3 MeV gammas provide the most intense prompt and delayed signals from photofission, but this is also the range of energies where most natural gamma backgrounds exist. In addition, the scattering of the gamma source beam will contribute a (prompt) background at all gamma energies. Additional experiments (via accelerated proton beams) and modeling (via Monte Carlo radiation transport simulations) will be performed to more accurately assess the impact of these backgrounds on detectability and the generation of false-positive signals. A preliminary conclusion that can be reached from the calculations performed so far is that the prompt neutrons and delayed gamma-ray signatures may provide the best signal from induced photofission of shielded nuclear material.

5. SUMMARY

The FIND active interrogation system will be based on a Gamma Tube photon source using low-energy proton-induced nuclear reactions to produce high intensities of mono-energetic gamma rays that can induce fission in nuclear materials followed by detection of the emitted radiation signatures. When realized, this source will be simpler, more cost effective, more efficient, and easier to scale than comparable high-energy accelerator alternatives. Our LDRD research has focused on the preliminary assessment of the viability of this concept through a program of experiments and simulations that determines the performance limits of a fully field deployable interrogation system. In particular, we have identified lanthanum hexaboride (LaB_6) and boron carbide (B_4C) as the leading target materials for the Gamma Tube. We have also demonstrated the detection of photofission signatures from depleted uranium. Through accelerator experimentation, we have identified the prompt neutron and delayed gamma-ray emissions as the best signals for detecting shielded SNM. Full development of the Gamma Tube will lead to the following important improvements over other source types: 1) low-energy nuclear reactions are used to produce high yields of monochromatic gamma-rays, 2) virtually all of the generated gamma-rays are “photofission worthy”, i.e., the gamma-ray energies coincide with the peak of the photofission cross section (in contrast, only a small fraction of bremsstrahlung photons can stimulate photofission), and 3) by stacking multiple units together, the resulting “linear gamma source” can be made to almost any length which is not as easily accomplished with large accelerator-based systems.

6. REFERENCES

- [1] J. Verbeke, A.S. Chen, J. L. Vujic, and K.N. Leung, Nucl. Tech. **134** (2001) 278; J. Verbeke, J. L. Vujic, and K.N. Leung, Nucl. Tech. **129** (2000) 257.
- [2] L.C. Feldman and S.T. Picraux, in *Ion Beam Handbook for Material Analysis* (J.W. Mayer and E. Rimini, editors), Academic Press, Inc., New York (1977).
- [3] R.G. Herb, D.W. Kerst, and J.L. McKibben, Phys. Rev., **51**(9) (1937) 691.
- [4] D.R. Tilley, C.M. Cheves, J.L. Godwin, G.M. Hale, H.M. Hofmann, J.H. Kelley, G. Sheu, H.R. Weller, “Energy Levels of Light Nuclei, A=3-20”, URL <http://www.tunl.duke.edu/nucldata>
- [5] P.M. Endt, Nucl. Phys., **A521** (1990) 1.
- [6] S. Harissopoulos, C. Chronidou, K. Spyrou, T. Paradellis, C. Rolfs, W.H. Schulte, and H.W. Becker, Eur. Phys. J. A, **9** (2000) 479.
- [7] S. Croft, Nucl. Instr. Meth. **A307** (1991) 353.
- [8] L. Ricken, K. Bodek, and A. Szczerba, Nucl. Phys. **A515** (1990) 226.
- [9] R.C. Weast, *CRC Handbook of Chemistry and Physics*, CRC Press, Inc., Boca Raton, Florida (1987).
- [10] E.B. Norman et al., Nucl. Instr. Meth. **A521** (2004) 608.
- [11] B. MacFarlane and M. White, “IAEA Photonuclear Data”, URL <http://t2.lanl.gov/data/photonuclear.html>
- [12] Dennis Slaughter *et al.*, LLNL Report UCRL-ID-155315 (2003).
- [13] G.R. Keepin, LANL Report LA-4457-MS (1970).
- [14] J.L. Jones *et al.*, Nucl. Instr. Meth. **B241** (2005) 770.
- [15] J.L. Jones *et al.*, Application of Accelerators in Research and Industry: 17th Int'l. Conference (J.L. Duggan and I.L. Morgan, editors) AIP Conference Proceedings, Vol. 680, Melville, New York (2003) 947.
- [16] C.E. Moss, C.A. Goulding, C.L. Hollas, and W.L. Myers, Application of Accelerators in Research and Industry: 17th Int'l. Conference (J.L. Duggan and I.L. Morgan, editors) AIP Conference Proceedings, Vol. 680, Melville, New York (2003) 900.

Distribution

5	1056	Barney Doyle, 1111
1	1421	Paula Provencio, 1111
1	1427	Julia Phillips, 1100
1	9004	William Ballard, 8200
1	9004	Patricia Falcone, 8110
1	9004	Jill Hruby, 8100
1	9004	Carolyn Pura, 8126
1	9004	Paul Rockett, 8158
1	9041	Ronald Stoltz, 8158
1	9042	Tony Chen, 8776
1	9042	Mike Chiesa, 8774
1	9161	Bill Even, 8760
1	9402	F. Patrick Doty, 8772
10	9402	Arlyn Antolak, 8772
1	9402	John Goldsmith, 8772
5	9402	Daniel Morse, 8772
1	9404	Art Pontau, 8750
1	9405	Davina Kwon, 8770
1	9405	Robert Carling, 8700
1	9915	James Wilhelm, 8529
1	9956	Kristin Hertz, 8772
2	0899	Technical Library, 9616
2	9018	Central Technical Files, 8945-1
1	0188	D. Chavez, LDRD Office, 1030